

**Constructive effects of noise in homoclinic chaotic systems**C. S. Zhou,<sup>1</sup> J. Kurths,<sup>1</sup> E. Allaria,<sup>2</sup> S. Boccaletti,<sup>2</sup> R. Meucci,<sup>2</sup> and F. T. Arecchi<sup>2,3</sup><sup>1</sup>*Institute of Physics, University of Potsdam, PF 601553, 14415 Potsdam, Germany*<sup>2</sup>*Istituto Nazionale di Ottica Applicata, Largo E. Fermi, 6, I50125 Florence, Italy*<sup>3</sup>*Department of Physics, University of Florence, Florence, Italy*

(Received 3 January 2003; published 27 June 2003)

Many chaotic oscillators have coherent phase dynamics but strong fluctuations in the amplitudes. At variance with such a behavior, homoclinic chaos is characterized by quite regular spikes but strong fluctuation in their time intervals due to the chaotic recurrence to a saddle point. We study influences of noise on homoclinic chaos. We demonstrate both numerically and experimentally on a CO<sub>2</sub> laser various constructive effects of noise, including coherence resonance, noise-induced synchronization in uncoupled systems and noise-enhanced phase synchronization, deterministic resonance with respect to signal frequency, and stochastic resonance versus noise intensity in response to weak signals. The peculiar sensitivity of the system along the weak unstable manifold of the saddle point underlines the unified mechanism of these nontrivial and constructive noise-induced phenomena.

DOI: 10.1103/PhysRevE.67.066220

PACS number(s): 05.45.Xt, 05.40.Ca

**I. INTRODUCTION**

Resonant response of a nonlinear system to a weak driving signal has been investigated in various contexts. In a self-sustained periodic oscillator, the system adjusts its time scale, achieving frequency and phase locking to the driving signal. This phenomenon of deterministic resonance, characterized by an Arnold tongue synchronization region in the parameter space of the amplitude and frequency of the driving signal, is of fundamental importance for applications in various fields [1]. Recently, the study of phase synchronization (PS) has been extended to chaotic oscillators [2–6] and found in chemical [7], laser [8], and other [9] experimental systems. For example, in the chaotic and phase-coherent Rössler oscillator, a phase variable can be defined, which is associated with the time scales of the oscillations, e.g., the return time  $T$  between two successive crossings of a Poincaré section [4]. This system displays very coherent phase dynamics due to a small fluctuation of  $T$ , although the amplitudes fluctuate strongly. As a result, PS occurs when the chaotic oscillator is periodically driven by a weak external signal [2,4] or when two nonidentical oscillators are weakly coupled [3], while the amplitudes remain chaotic and often uncorrelated. This property of coherent phase dynamics and in parallel strong chaotic fluctuation of amplitudes is quite general in chaotic oscillations, resulting from a period-doubling bifurcation [10], and PS occurs similar to coupled periodic oscillators. With strong enough coupling, both the phase and amplitude may become synchronized and we observe almost complete synchronization [11].

Noise may influence synchronization in different ways. Usually, it has a degrading effect, as especially inducing phase slips and smearing out the border of the synchronization region that shrinks for increasing noise intensity [12]. Similarly, noise induces phase slips of locked chaotic oscillators [13]. In complete synchronization of coupled chaotic systems, very small noise may result in a large intermittent loss of synchronization due to transversely unstable invariant sets in the synchronization manifold [14].

On the other hand, noise may play constructive effects in nonlinear systems through stochastic resonance (SR) [15] or coherence resonance (CR) [16]. A bistable or excitable system can generate a coherent response to a subthreshold external stimulus in the presence of a suitable amount of noise. The coherence is maximal at a certain optimal noise intensity. Stochastic resonance has also been studied from the viewpoint of noise-enhanced synchronization of the switching events to the external signal, because noise controls the average switching rate of the system and the response is optimal when it is close to that of the external signal [17–19]. This resonance behavior, however, is not the same as deterministic resonance in coupled self-sustained oscillators: while the synchronization exhibits a resonancelike behavior with a change of the noise intensity at a fixed driving frequency, it does not display resonancelike behavior as a function of the driving frequency [19]. When the driving signal fluctuations are much slower than all system time scales, the signal-to-noise ratio is independent of signal frequencies, while it shows a sensitivity to higher signal frequencies in excitable systems [20,21]. With CR pure noise alone can generate the most coherent motion without an external signal, as observed in excitable systems [16]. Internal noise due to ion channel activity can generate SR and CR in the collective behavior of channel ensembles [22]. In coupled excitable elements, noise or parameter disorder can enhance CR through phase synchronization of the spiking sequence of the elements [23]. In phase-coherent chaotic oscillators, noise may also play a constructive role to enhance PS in the weak coupling regime [24].

Two identical systems, which are not coupled but subjected to a common noise, may synchronize, as has been reported both in periodic [25] and in chaotic [26] cases. For noise-induced synchronization (NIS) to occur, the largest Lyapunov exponent (LLE) ( $\lambda_1 > 0$  in chaotic systems) has become negative [26]. However, whether and how noise can induce synchronization of chaotic systems has been a subject of intense controversy [27–31]. The debate mainly focuses on the effect of the mean value of noise [30,31]. It has been

shown that a nonzero mean (biased) noise plays a decisive role by shifting the dynamics toward a stable regime [30,31]. However, the general conclusion [31] that an unbiased noise cannot lead to synchronization has been disproved by recent examples [32]. We have recently clarified this long-standing controversy by showing that the key mechanism of NIS is the existence in phase space of a large *contraction region*, where nearby trajectories converge to each other [33]. Noise changes the competition between contraction and expansion, and synchronization ( $\lambda_1 < 0$ ) occurs if contraction becomes dominant. However, in the systems of Refs. [32,33], the dynamical structure has been significantly deformed when NIS occurs at large enough noise intensity. So far, it is not known in what types of systems a significant contraction region can exist and NIS occurs, while the basic dynamical structure is mainly preserved in the presence of noise.

Common noise is of great relevance in several disciplines, especially in neuroscience. Neurons connected to another group of neurons receive a common input signal, which often approaches a Gaussian distribution as a result of integration of many independent synaptic currents. A common external noise can generate stochastic phase synchronization of bursts induced by internal noise in noncoupled sensory neurons [34]. Experiments on rat neocortical neurons have demonstrated a remarkable reliability of spike timing in response to a fluctuating stimulus [35]. When the input is a constant current, a neuron generates independent spike trains in repeated experiments, and desynchronization of corresponding spikes increases over the course of the stimulus. Remarkably, when a strong enough Gaussian noise is input in addition to the constant current, the neuron generates repetitive spike trains in repeated experiments with the same fluctuating stimulus. The dynamical mechanism underlying such a response of neurons, however, has not been fully understood. One possible explanation is based on ion channel noise [36]. Recently, numerical simulations with a stochastic Hodgkin-Huxley (HH) model have shown that ion channel noise may be significant for the reliability and precision of spike timing, especially when the number of ion channels that are open near the threshold for spike firing is small, while a deterministic HH model generates regular (periodic) and jitter spike trains in response to the constant and fluctuating input, respectively [37]. Spiking behavior of a single neuron may be described already rather accurately by a deterministic model because of the large number of excitable ion channels [38]. From the viewpoint of deterministic dynamics, the highly unreliable spiking trains in response to a constant current may be attributed to chaotic firing starting from nearby initial conditions (quiescent states), and reliable response to fluctuating current may be regarded as NIS of neurons. Clearly, studying NIS of chaotic dynamical systems, especially in those displaying spiking behavior similar to the unreliable spiking of neurons in response to constant current, may be of relevance to this important problem of information encoding by spike timing in neuroscience.

Synchronization due to a random forcing is also of great relevance in ecology. Two separated populations may become correlated when exposed to similar environmental fluctuations, known as the Moran effect [39]. Observations have

shown a synchronous fluctuation of populations over large geographical regions [40,41]. However, the Moran effect is only well understood in linear and simple systems, but not in nonlinear ones [42], especially, it was pointed out that for chaotic models, the Moran effect alone cannot synchronize populations [43]. It is thus important to investigate the mechanism beyond noise-induced synchronization.

Homoclinic chaos [44] represents a class of self-sustained chaotic oscillations that exhibit quite different behavior as compared to phase coherent chaotic oscillations. Typically, these chaotic oscillators possess the structure of a saddle point  $S$  embedded in the chaotic attractor. The chaotic trajectories starting from a neighborhood of  $S$  leave  $S$  slowly along the unstable manifold and have a fast and close recurrence to  $S$  along the stable manifold after a large excursion (spike). Thus a significant contraction region exists close to the stable manifold. The dynamics is characterized by a sequence of spikes with widely fluctuating time intervals  $T$ . Such a structure underlies spiking behavior in many neuron [38,45], chemical [46], laser [47], and El Niño [48] systems. It is important to note that this dynamics is highly nonuniform, in the sense that the sensitivity to small perturbations is high only in the vicinity of  $S$  along the unstable directions. A weak noise thus may influence  $T$  significantly.

In this paper we study noise effects on homoclinic chaos. We find that weak noise can enhance the coherence of the spike train. As a result, the LLE becomes negative and a weak common noise can induce complete synchronization of identical uncoupled systems. These noise-induced changes also enhance strongly the response of the system to a weak signal. The noisy systems display resonances with respect to both the noise intensity and the signal frequency. A brief account of the results on noise-enhanced phase synchronization has been published in a recent Rapid Communication [49].

The paper is organized as follows. In Sec. II we describe the experimental laser system and the model equations. In Sec. III we discuss the dynamical features of the system and noise-induced changes in time scale, and demonstrate coherence resonance. Noise-induced complete synchronization of two lasers is presented in Sec. IV. Section V considers noise-enhanced phase synchronization to a weak signal, and Sec. VI demonstrates stochastic resonance. Finally, the results are summarized in Sec. VII.

## II. THE SYSTEM

We demonstrate these nontrivial effects of noise in a single mode CO<sub>2</sub> laser, both experimentally and numerically. The experimental setup consists of a CO<sub>2</sub> laser with an intracavity loss modulator, driven by a feedback signal, which is proportional to the laser output intensity. The system is operating in a homoclinic chaos regime where the laser output consists of a chaotic sequence of spikes [47,50]. To investigate the role of external noise, a Gaussian noise generator is inserted into the feedback loop. The noise generator has a high frequency cutoff at 50 kHz, but for all purposes it can be regarded as a white noise source.

We carry out numerical simulations on the model [50]

$$\dot{x}_1 = k_0 x_1 (x_2 - 1 - k_1 \sin^2 x_6), \quad (1)$$

$$\dot{x}_2 = -\gamma_1 x_2 - 2k_0 x_1 x_2 + g x_3 + x_4 + p_0, \quad (2)$$

$$\dot{x}_3 = -\gamma_1 x_3 + g x_2 + x_5 + p_0, \quad (3)$$

$$\dot{x}_4 = -\gamma_2 x_4 + z x_2 + g x_5 + z p_0, \quad (4)$$

$$\dot{x}_5 = -\gamma_2 x_5 + z x_3 + g x_4 + z p_0, \quad (5)$$

$$\dot{x}_6 = -\beta \left( x_6 - b_0 + \frac{r x_1}{1 + \alpha x_1} \right) + D \xi(t). \quad (6)$$

Here,  $x_1$  represents the laser output intensity,  $x_2$  the population inversion between the two resonant levels,  $x_6$  the feedback voltage signal that controls the cavity losses, while  $x_3$ ,  $x_4$ , and  $x_5$  account for molecular exchanges between the two levels resonant with the radiation field and the other rotational levels of the same vibrational band. Furthermore,  $k_0$  is the unperturbed cavity loss parameter,  $k_1$  determines the modulation strength,  $g$  is a coupling constant,  $\gamma_1, \gamma_2$  are population relaxation rates,  $p_0$  is the pump parameter,  $z$  accounts for the number of rotational levels, and  $\beta, r, \alpha$  are, respectively, the bandwidth, the amplification, and the saturation factors of the feedback loop. With the following parameters  $k_0 = 28.5714$ ,  $k_1 = 4.5556$ ,  $\gamma_1 = 10.0643$ ,  $\gamma_2 = 1.0643$ ,  $g = 0.05$ ,  $p_0 = 0.016$ ,  $z = 10$ ,  $\beta = 0.4286$ ,  $\alpha = 32.8767$ ,  $r = 160$ , and  $b_0 = 0.1031$ , the model reproduces very well the regime of homoclinic chaos observed experimentally. The previous study [50] did not take into account small intrinsic noise present in the experimental system. We have measured the noise in the feedback variable ( $x_6$ ) in the case when the laser is turned off. This enables us to estimate an intrinsic noise rms amplitude  $D \approx 7$  mV, which is about 0.14% of the feedback signal  $x_6$  in the experimental system. In the model,  $D = 0.0005$  is equivalent to the intrinsic noise amplitude in  $x_6$ .

The model is integrated by using a Heun algorithm [51] with a small time step  $\Delta t = 5 \times 10^{-5}$  ms (note that typical  $T \sim 0.5$  ms).

### III. NOISE-INDUCED CHANGES IN TIME SCALE AND COHERENCE RESONANCE (CR)

Without added noise, the laser output displays large spikes, followed by a fast damped train of a few oscillations towards the saddle point  $S$  and a successive longer train of growing oscillations spiraling out from  $S$  [Fig. 1(a)]. The damped oscillation manifests a strong contraction along the stable manifold in the phase space, while the growing one manifests weak expansion along the unstable manifold [Fig. 1(b)], which can be described approximately as

$$X(t) \sim X_0 \exp[\lambda_u(t - t_0)] \cos \omega(t - t_0), \quad (7)$$

where  $\lambda_u \pm i\omega$  are the eigenvalues of the unstable manifold of  $S$  and  $X_0$  is the distance from  $S$  at any reinjection time  $t_0$ . Thus, the smaller  $X_0$  is, the longer is the time taken to spiral

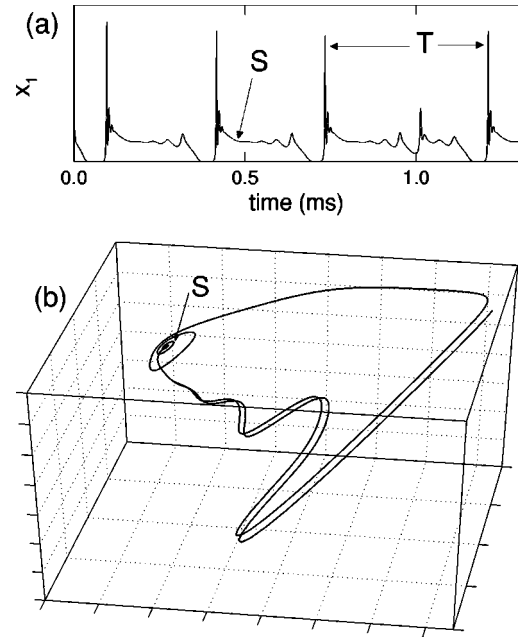


FIG. 1. (a) Laser output intensity  $x_1$  of the noise-free model. (b) Orbits in the 3D phase space  $(x_1, x_2, x_6)$ .

out. The model displays a broad range of time scales. There are many peaks in the distribution  $P(T)$  of  $T$ , as shown in Fig. 2(a). In the presence of noise, the trajectory on average cannot come closer to  $S$  than the noise level and perform those oscillations very close to  $S$ . With a larger  $X_0$ , the system spends a shorter time following the guidance of the unstable manifold.

A small noise ( $D = 0.0005$ ) changes significantly the time scales of the model.  $P(T)$  is now characterized by a dominant peak followed by a few exponentially decaying ones [Fig. 2(b)]. This distribution of  $T$  is typical for small  $D$  in the range  $D = 0.00005 - 0.002$ . The experimental system with only intrinsic noise (equivalent to  $D = 0.0005$  in the model) has a very similar distribution  $P(T)$  (not shown). At the larger noise intensity  $D = 0.01$ , the fine structure of the peaks is smeared out and  $P(T)$  becomes a unimodal peak in a smaller range [Fig. 2(c)]. Note that the mean value  $T_0(D) = \langle T \rangle_t$  (Fig. 2, vertical dotted lines) decreases with  $D$ . When the noise is rather large, it affects the dynamics not only close to  $S$  but also during the spiking, so that the spike sequence becomes fairly noisy. We observe the most coherent spike sequences at a certain intermediate noise intensity, as seen in Figs. 3(c) and 3(d), showing the laser output of the

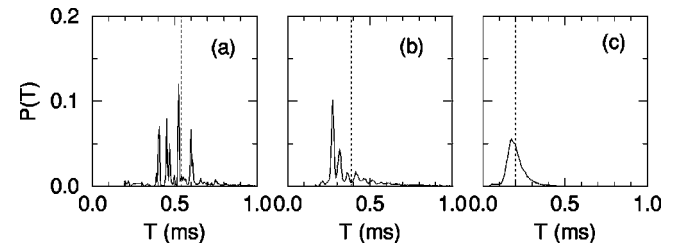


FIG. 2. Noise-induced changes in time scales. (a)  $D = 0$ , (b)  $D = 0.0005$ , and (c)  $D = 0.01$ . The dotted lines show the mean inter-spike interval  $T_0(D)$ , which decreases with increasing  $D$ .

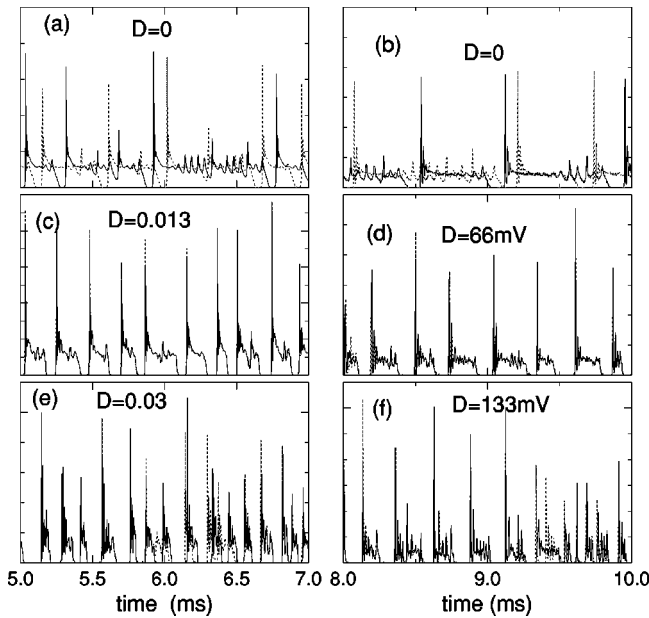


FIG. 3. Time series of output intensities (arbitrary units) of two lasers  $x_1$  (solid lines) and  $y_1$  (dotted lines) with a common noise. Left panel (a),(c),(e): model systems including independent noise (amplitude  $D_1=0.0005\sim$ intrinsic noise level). Right panel (b),(d), (f): experimental system.

model and the experimental systems, respectively. The system takes a much shorter time to escape from  $S$  after the fast reinjection, and the main structure of the spike is preserved. We quantify the coherence by  $R$  [16],

$$R = T_0(D) / \sigma_T, \quad (8)$$

where  $\sigma_T$  is the standard deviation of  $P(T)$ . When  $D$  increases,  $R$  reaches a maximal value and decreases again [Figs. 4(a) and 4(b)]. Hence it exhibits CR [16], both in the model and the experimental systems.

The mechanism of CR in homoclinic chaotic systems is quite different from that in excitable systems [16]. Excitable systems are stable at a fixed point, and noise can kick the system over a threshold to generate a spike, which returns back to the fixed point after a refractory period. CR is a result of the competition between the noise-controlled escaping time over the threshold and the refractory period, which is affected only when noise becomes rather strong. Homoclinic chaotic systems are already in an oscillatory regime and the spike sequence is generated by a chaotic recurrence

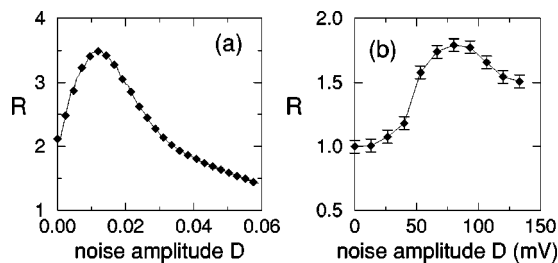


FIG. 4. Coherence resonance (CR) in model (a) and experimental (b) systems.

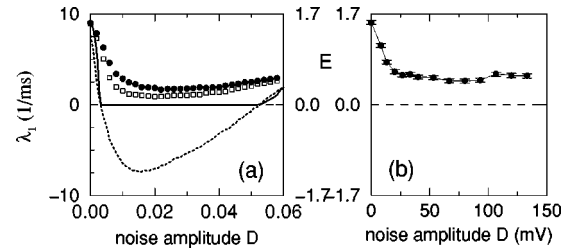


FIG. 5. Noise-induced synchronization (NIS) in model (a) and experimental (b) systems. (a) Dotted line: the LLE  $\lambda_1$ . Solid line: normalized synchronization error  $E$  between two fully identical laser models  $x$  and  $y$ . Closed circles:  $E$  between two lasers with a small independent noise (intensity  $D_1=0.0005$ ). Open squares:  $E$  between two nonidentical lasers with  $b_0=0.1031$  and  $b_0=0.1032$  vs amplitude  $D$  of the common noise.

to the saddle  $S$ . CR occurs as a consequence of a small noise that changes the time spent in the neighborhood of  $S$  along the weak unstable manifold. The coherence is lost when strong noise also affects the dynamics during the reinjection along the stable manifold. A property common to homoclinic chaos and excitable systems is the separation of time scales so that the fast motion is hardly influenced by weak noise. Note that this mechanism is also different from noise-induced coherent jumping among coexisting attractors [52].

#### IV. NOISE-INDUCED COMPLETE SYNCHRONIZATION (NIS)

Since noise reduces the time spent by the system following the guidance of the unstable manifold, the degree of expansion is reduced. This changes the competition between contraction and expansion, and contraction may become dominant at large enough  $D$ . To measure these changes, we calculate the LLE  $\lambda_1$  in the model as a function of the noise intensity  $D$  [Fig. 5(a), dotted line].  $\lambda_1$  undergoes a transition from a positive to a negative value at  $D_c \approx 0.0031$ . Beyond  $D_c$ , two identical laser models  $x$  and  $y$  with different initial conditions but the same noisy driving  $D\xi(t)$  achieve complete synchronization after a transient, as shown by the vanishing normalized synchronization error  $E = \langle |x_1 - y_1| \rangle / \langle |x_1 - \langle x_1 \rangle| \rangle$  [Fig. 5(a), solid line]. At larger noise intensities, expansion becomes again significant, and the LLE increases and synchronization is lost when  $\lambda_1$  becomes positive for  $D > 0.052$ . Notice that even when  $\lambda_1 < 0$ , the trajectories still have access to the expansion region where small distances between them grow temporally. As a result, when the systems are subjected to additional perturbations, synchronization is lost intermittently, especially for  $D$  close to the critical values. Actually, in the experimental laser system, there always exists a small intrinsic noise source. To take into account this intrinsic noise in real systems, we introduce into the equations  $x_6$  an equivalent amount of independent noise (with amplitude  $D_1=0.0005$ ) in addition to the common one  $D\xi(t)$ . By comparison, it is evident that the sharp transition to a synchronized regime in fully identical model systems [Fig. 5(a), solid line] is smeared out [Fig. 5(a), closed circles]. The parameter mismatch has similar desynchroniz-



ing effects, as shown by  $E$  between two lasers in the homoclinic regime, with  $b_0=0.1031$  and  $b_0=0.1032$ , but the same random forcing [Fig. 5(a), open squares]. In our experimental study of NIS, for each noise intensity  $D$  we repeat the experiment twice with the same external noise. As consistent with numerical results with small independent noise,  $E$  does not reach zero due to the intrinsic noise, and it increases slightly at large  $D$  [Fig. 5(b)].

It is important to emphasize that NIS and CR are obtained for rather small noise. In particular, the onset of NIS occurs at an experimental added noise ( $D \approx 20$  mV) of about 0.42% of the feedback signal  $x_6$ , whereas the maximal coherence is obtained for a noise ( $D \approx 66$  mV) of about 1.3% of the feedback signal. This tiny amount of noise only affects the system's behavior close to the saddle  $S$ , while it does not change the main geometrical feature of the spike. This feature is also similar to neuron spiking in the presence of a fluctuating signal where the shape of the spikes is preserved, while the interspike intervals are altered. This is important for biological information processing.

A more descriptive view of NIS and CR is shown in Fig. 3 by some portions of the numerical (a), (c), (e) and experimental (b), (d), (f) laser intensity data for three noise intensities. Precisely, Figs. 3(a) and 3(b) are obtained without a common noise, Figs. 3(c) and 3(d) for the noise value  $D_{max}$  at which the coherence factor  $R$  is maximal, and Figs. 3(e) and 3(f) are obtained for a noise intensity  $D \approx 2D_{max}$ . In the absence of a common noise, the two signals are unsynchronized, the spike intervals  $T$  are large on average and fluctuate strongly. For  $D \approx D_{max}$ , both experimental and numerical results demonstrate the existence of almost complete synchronization induced by the external noise, and in parallel the spike sequences are most coherent with a smaller average  $T$ , because the escaping time from the vicinity of the saddle  $S$  has been reduced; yet, the main geometry of the spikes is preserved. Finally, at a larger noise, synchronization is intermingled with short epochs of desynchronization. All features of NIS and CR in the model and in the experimental system are in good agreement.

Our results again disprove previous claims that NIS can be achieved only by noise with a nonzero mean value [30,31], and verify that a significant contraction region plays the decisive role [33].

It is important to stress that a significant contraction region exists generically in homoclinic chaotic systems due to the strong stable manifold of the saddle  $S$ , so that we can expect NIS to occur at rather small noise intensities. In fact, we have also demonstrated NIS and CR in other homoclinic chaotic models, such as a chaotic HH model of thermally sensitive neurons. This model mimics various types of spike train patterns in electroreceptors from dogfish and catfish, and from facial cold receptors and hypothalamic neurons of the rat [53], and it has been demonstrated to display homoclinic bifurcation when the control parameter, the temperature, is varied [45]. Our simulations with this model also find NIS at rather small noise intensity and maximal coherence at a stronger intensity in a wide parameter range [54]. There NIS and CR have been examined in the collective response in ensembles of uncoupled or weakly coupled het-

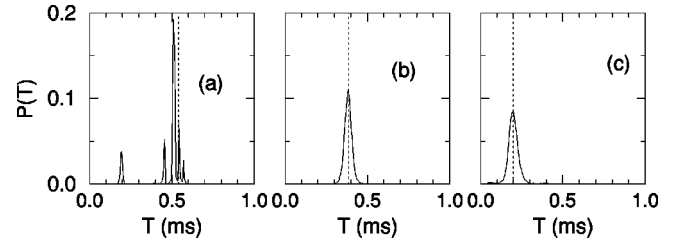


FIG. 6. Response of the laser model to a weak periodic signal [Eq. (9),  $A=0.01$ ] at various noise amplitudes. (a)  $D=0$ , (b)  $D=0.0005$ , and (c)  $D=0.01$ . The signal period  $T_e$  in (a), (b), and (c) corresponds to the mean interspike interval  $T_0(D)$  of the unforced model ( $A=0$ ), respectively (dotted lines in Fig. 2).

erogeneous neurons to a common fluctuating signal, in the context of spiking reliability and variability in neurobiology.

## V. NOISE-ENHANCED PHASE SYNCHRONIZATION AND DETERMINISTIC RESONANCE

Now we study how the noise-induced changes in the time scale affect the response of the system to a weak external driving signal. In the model and the experimental systems, the pump parameter  $p_0$  is now modulated as

$$p(t) = p_0[1 + A \sin(2\pi f_e t)], \quad (9)$$

by a periodic signal with a small amplitude  $A$  and a frequency  $f_e$ .

Phase synchronization of the laser to the signal has been studied recently [55]. Here, we focus on the constructive effects of noise on phase synchronization. To examine phase synchronization due to the driving signal, we compute the phase difference  $\theta(t) = \phi(t) - 2\pi f_e t$ . Here, the phase  $\phi(t)$  of the laser spike sequence is defined as [4]

$$\phi(t) = 2\pi \left( k + \frac{t - \tau_k}{\tau_{k+1} - \tau_k} \right) \quad (\tau_k \leq t < \tau_{k+1}), \quad (10)$$

where  $\tau_k$  is the spiking time of the  $k$ th spike, i.e., the spikes are used as marker events.

As a result of noise-induced changes in the time scales, the model displays quite different responses to a weak signal ( $A=0.01$ ) with a frequency  $f_e = f_0(D) = 1/T_0(D)$  [ $T_0(D) = \langle T \rangle_t$  at  $A=0$ ], i.e., equal to the mean spiking rate of the unforced model. At  $D=0$ ,  $P(T)$  of the forced model still has many peaks [Fig. 6(a)]. Phase slips occur frequently and the phase of the laser model is not locked by the external forcing (Fig. 7); while at  $D=0.0005$ ,  $T$  is sharply distributed around the signal period  $T_e = T_0(D)$  [Fig. 6(b)] and phase slips occur very rarely, i.e., phase locking becomes almost perfect. At a larger intensity  $D=0.01$ ,  $P(T)$  becomes lower and broader again [Fig. 6(c)] and several randomlike phase slips occur.

We have investigated systematically the response sensitivity of the laser model by analyzing the synchronization region (1:1 response) in the parameter space of the driving amplitude  $A$  and the relative initial frequency difference  $\Delta\omega = [f_e - f_0(D)]/f_0(D)$ , where the average frequency

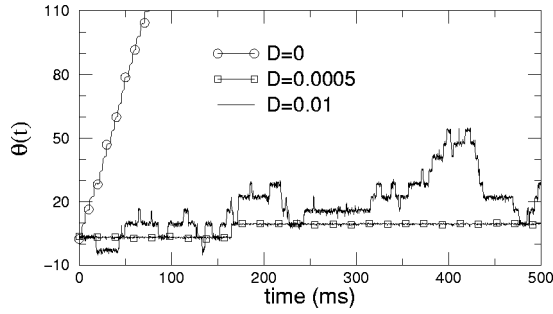


FIG. 7. Phase synchronization of the laser model to a weak driving signal at various noise intensities  $D$ .

$f_0(D)$  of the unforced laser model is an increasing function of  $D$ . The actual relative frequency difference in the presence of the signal is calculated as  $\Delta\Omega = (f - f_e)/f_0(D)$ , where  $f = 1/\langle T \rangle$  is the average spiking frequency of the forced laser model. The synchronization behavior of the noise-free model is quite complicated and unusual [Fig. 8(a)]. At weak amplitude (about  $A < 0.012$ ), there does not exist a tongue-like region similar to the Arnold tongue in periodically driven periodic oscillators or phase coherent chaotic ones; for a fixed  $A$ ,  $\Delta\Omega$  is not a monotonous function of  $\Delta\omega$  and vanishes only at some specific signal frequencies; at stronger driving amplitudes (about  $A > 0.012$ ), the system becomes periodic at a large frequency range. The addition of a small noise,  $D = 0.0005$ , drastically changes the response. Now, a tongue-like region [Fig. 8(b)], where effective frequency locking ( $|\Delta\Omega| \leq 0.003$ ) occurs, can be observed similar to that in usual noisy phase coherent oscillators. Synchronization is enhanced further at  $D = 0.001$ . At a stronger noise intensity  $D = 0.005$ , noise dominates over the weak signal in the vicinity of the saddle  $S$ , and the synchronization region shrinks, although the coherence  $R$  of the unforced system increases up to  $D \approx 0.013$  [Fig. 3(a)].

This very complicated and unusual response to a weak driving signal in the noise-free model, however, has not been observed in the experimental system [55]. This is due to the intrinsic noise whose amplitude is equivalent to  $D = 0.0005$  in the model. Very interestingly, synchronization in the experiment can also be enhanced further by adding external noise, especially for  $\Delta\omega > 0$ . However, an external noise too strong degrades synchronization again [Fig. 9(b)]. A comparison of numerical and experimental results for a similar noise range shows a good qualitative agreement (Fig. 9).

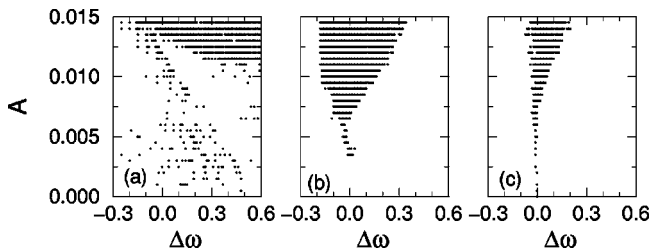


FIG. 8. Synchronization region of the laser model at various noise intensities. A dot is plotted when  $|\Delta\Omega| \leq 0.003$ . (a)  $D = 0$ , (b)  $D = 0.0005$ , and (c)  $D = 0.005$ .

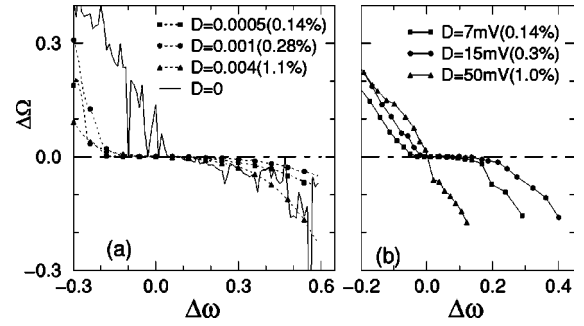


FIG. 9. Noise-enhanced PS: a comparison between the model and the experimental systems. (a) Model,  $A = 0.01$ . (b) Experiment: signal amplitude 10 mV ( $A = 0.01$ ); the noise amplitude denotes total noise measured in the feedback loop, and  $D = 7$  mV corresponds to the intrinsic noise. In both cases, the noise intensities are also indicated in % of the feedback signal  $x_6$ .

Thus, noise can play a constructive role to enhance frequency locking and PS of homoclinic chaos to a weak driving signal. Without noise, the model system exhibits a very complicated and unusual response to the signal due to a broad distribution of time scales; whereas in the presence of a small noise, it obtains a dominant time scale and displays a resonance versus the frequency, as in usual phase-coherent oscillators.

Furthermore, the PS behavior is optimized at a certain noise intensity as SR [15,17–19]. In the following, we study in detail how this SR is affected by the noise intensity  $D$ .

## VI. STOCHASTIC RESONANCE (SR)

First, we compute the dimensionless phase diffusion  $D_\theta$  as a function of the noise amplitude  $D$ , namely,

$$D_\theta = \frac{1}{2\pi f_0(D)} \frac{1}{2} \frac{d}{dt} [\langle \theta^2(t) \rangle - \langle \theta(t) \rangle^2]. \quad (11)$$

$D_\theta$  measures the spreading of an initial distribution of the phase difference with the evolution of time. The degree of synchronization is higher for smaller  $D_\theta$  (phase is locked on average for  $n = 2\pi/D_\theta$  periods [19]). In Fig. 10, both  $\Delta\Omega$  and  $D_\theta$  are shown as functions of  $D$  for  $A = 0.01$  and various relative initial frequency differences  $\Delta\omega$ . Stochastic resonance of phase synchronization is indicated clearly by the minimum of  $D_\theta$  at a certain noise intensity. Note that for a

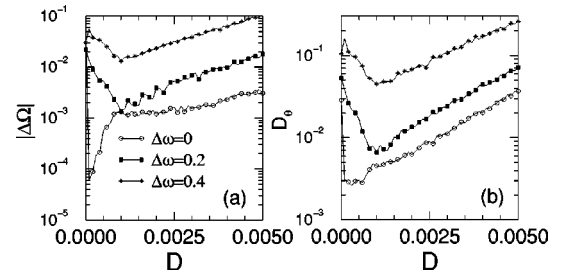


FIG. 10. Relative frequency difference  $\Delta\Omega$  (a) and phase diffusion  $D_\theta$  (b) as a function of the noise amplitude  $D$  for various fixed relative initial frequency differences  $\Delta\omega$ .  $A = 0.01$ .

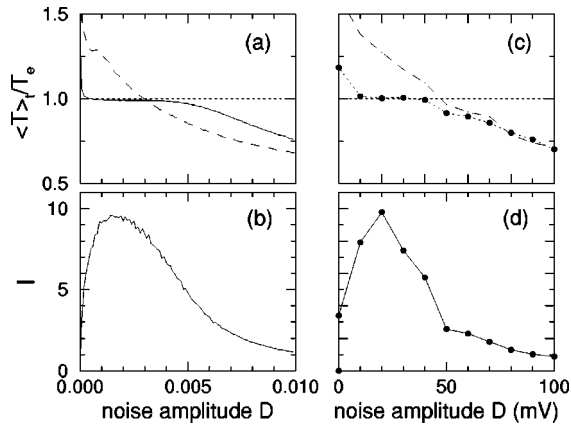


FIG. 11. Stochastic resonance for a fixed driving period. Left panel: model,  $A=0.01$ ,  $T_e=0.3$  ms. Right panel: experiment, forcing amplitude 10 mV ( $A=0.01$ ) and period  $T_e=1.12$  ms; here  $D$  is the amplitude of the added external noise. Upper panel: noise-induced coincidence of average time scales (dashed line,  $A=0$ ) and the synchronization region. Lower panel: coherence  $I$  of the laser output.  $\alpha=0.1$  in Eq. (12).

fixed  $\Delta\omega$ , the driving frequency  $f_e$  is changing with  $D$ , and an enhanced response sensitivity relative to the average spiking frequency of the noisy system is a result of the noise-enhanced coherence of the time scales, as indicated by the sharpened distribution  $P(T)$  in Fig. 2(b).

We now study how the response is affected by  $D$  for a fixed signal period  $T_e$ . Here, in the unforced homoclinic chaotic lasers the average interspike interval  $T_0(D)$  decreases with increasing  $D$ , and SR similar to that in bistable or excitable systems can also be observed. We adopt the following measure of coherence as an appropriate indicator of stochastic resonance [21]:

$$I = \frac{T_e}{\sigma_T} \int_{(1-\alpha)T_e}^{(1+\alpha)T_e} P(T) dT, \quad (12)$$

where  $\alpha$  with  $0 < \alpha < 0.25$  is a free parameter. This indicator takes into account both the fraction of spikes with an interval roughly equal to the forcing period  $T_e$  and the jitter between spikes [21]. SR of the 1:1 response to the driving signal has been demonstrated both in the model and in the experimental systems by the ratio  $\langle T \rangle / T_e$  and  $I$  in Fig. 11. Again, the behavior agrees well in both systems. For  $T_e < T_0(0)$ , there exists a synchronization region where  $\langle T \rangle / T_e \approx 1$ . The noise amplitude optimizing the coherence  $I$  is smaller than that induces coincidence of  $T_0(D)$  and  $T_e$  [dashed lines in Figs. 11(a) and 11(c)]. It turns out that maximal  $I$  occurs when the dominant peak of  $P(T)$  [Fig. 2(b)] is located at  $T_e$ . For  $T_e > T_0(0)$ , noise may induce an  $n:1$  response, where the laser produces  $n$  spikes per signal period. For example, at  $T_e = 0.6$ , a 2:1 response can be observed in the laser model, which generates two spikes with alternate small and large intervals  $T_1$  and  $T_2$  satisfying  $T_1 + T_2 = T_e$ , as seen in Fig. 12. The  $n:1$  response also exhibits a locking region and SR with varying  $D$ . This kind of noise-induced synchronization has not been reported in usual stochastic resonance systems,

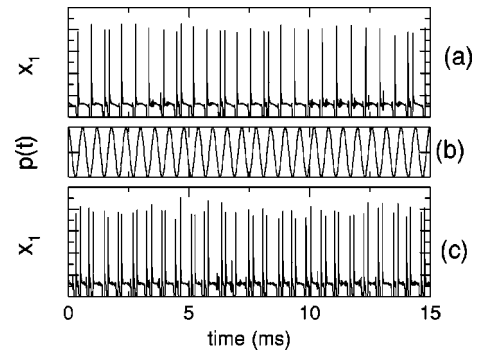


FIG. 12. Noise-enhanced 2:1 response of the laser model.  $A=0.01$ ,  $T_e=0.6$ . (a) Laser output  $x_1$  (arbitrary units) at  $D=0$ , (b) external signal, and (c)  $x_1$  at  $D=0.004$ .

where at large  $T_e$  numerous firings occur randomly per signal period and result in an exponential background in  $P(T)$  of the forced system, while at small  $T_e$  a 1: $n$  response may occur, which means an aperiodic firing sequence with one spike for  $n$  driving periods on average [15,20,21]. In both cases, the sequences are irregular.

The main results in Secs. V and VI have been presented recently [49]. Here a more quantitative examination of the synchronization degree by phase diffusion  $D_\theta$  (Fig. 10) shows that the enhanced synchronization and response to weak signals are consequences of the enhanced coherence in time scales shown in Sec. III. The more systematic and extensive investigation in this paper has revealed that the special sensitivity to noise along the weak unstable manifold of the saddle point acts as an unified mechanism for various nontrivial and constructive noise-induced phenomena in this general class of systems, which is quite different from those demonstrated previously in other systems.

## VII. CONCLUSION AND DISCUSSION

We have shown that in homoclinic chaotic systems characterized by a strong fluctuation of the interspike interval, a small amount of noise makes the time scales more regular, due to reduced residence time in the weak unstable region. Various constructive effects have been shown experimentally and demonstrated numerically as a consequence of this noise-induced change in the time scale. The system displays coherence resonance without an external signal and enhanced phase synchronization, deterministic resonance, and stochastic resonance in response to a weak signal.

Note that the response of the homoclinic chaos to noise, i.e., more regular spike intervals with a smaller mean value, is similar to the excitable systems where resonances with respect to both the signal frequency and the noise intensity can also be observed [20,56]. However, a noise-induced phase locking with respect to the signal frequency, especially for the  $n:1$  ratios, to our knowledge, has not been demonstrated in excitable systems for rather weak signal. In *coupled* excitable elements, similar locking behavior occurs due to the interplay between the coupling and the noise-induced excitations [57].

The phenomena of coherence resonance, noise-induced

synchronization, stochastic resonance and noise-enhanced phase synchronization demonstrated in this laser system have been documented previously in the literature, but separately in different systems with different mechanism for each phenomenon. In the homoclinic chaotic system, this peculiar property of the sensitivity to noisy perturbation in the weak unstable manifold acts as the unified mechanism for various nontrivial phenomena in a single system.

These findings should have a strong impact in neuroscience because a wide class of sensory neurons demonstrates homoclinic chaotic spiking activity [45,53]. Coexistence of conventional and stochastic resonances may be significant for information processing in biological systems insofar as noise enhances the sensitivity to both amplitude and frequency of the external signals.

It is important to emphasize that we have also shown that unbiased noise is sufficient to induce complete synchronization. Moreover, NIS is not necessarily associated with large noise intensities, but in the case of homoclinic chaos it can

be induced by weak noise that does not significantly alter the geometry of the dynamics. The contraction region associated with the saddle point is crucial for NIS. This mechanism of synchronization due to significant contraction regions may shed light in understanding of the population synchronization in ecology due to large-scale climate. The mechanism presented here may be important for the dynamics of neurons as one of the basic possibilities of interpretation of the experimental observation of the reliability and precision of spike timing of neurons [35]. While it is not known whether the neocortical neurons in Ref. [35] are deterministically chaotic or not, our findings should stimulate further studies in this direction.

#### ACKNOWLEDGMENTS

This work was supported by SFB555, the Humboldt-Foundation, and EC Network HPRN CT 2000 00158.

- 
- [1] Y. Kuramoto, *Chemical Oscillations, Waves and Turbulence* (Springer, Berlin, 1984).
- [2] E.F. Stone, *Phys. Lett. A* **163**, 367 (1992); A.S. Pikovsky *et al.*, *Physica D* **104**, 219 (1997).
- [3] M.G. Rosenblum, A.S. Pikovsky, and J. Kurths, *Phys. Rev. Lett.* **76**, 1804 (1996).
- [4] A.S. Pikovsky, M.G. Rosenblum, G.V. Osipov, and J. Kurths, *Physica D* **104**, 219 (1997).
- [5] A.S. Pikovsky, M.G. Rosenblum, and J. Kurths, *Synchronization—A Universal Concept in Nonlinear Sciences* (Cambridge University Press, Cambridge, 2001).
- [6] S. Boccaletti, J. Kurths, G. Osipov, D.L. Valladares, and C.S. Zhou, *Phys. Rep.* **366**, 1 (2002).
- [7] I.Z. Kiss and J.L. Hudson, *Phys. Rev. E* **64**, 046215 (2001); *Phys. Chem. Chem. Phys.* **4**, 2638 (2002); I.Z. Kiss, Y. Zhai, and J.L. Hudson, *Science* **296**, 1676 (2002).
- [8] D.Y. Tang *et al.*, *Chaos* **8**, 697 (1998); D.J. Deshazer *et al.*, *Phys. Rev. Lett.* **87**, 044101 (2001); K.V. Volodchenko *et al.*, *Opt. Lett.* **26**, 1406 (2001); N. Kravtsov *et al.*, *Quantum Electron.* **32**, 251 (2002).
- [9] D. Maza *et al.*, *Phys. Rev. Lett.* **85**, 5567 (2000); C.M. Ticos *et al.*, *ibid.* **85**, 2929 (2000).
- [10] B. Blasius, A. Huppert, and L. Stone, *Nature (London)* **399**, 354 (1999).
- [11] L.M. Pecora and T.L. Carroll, *Phys. Rev. Lett.* **64**, 821 (1990); M.G. Rosenblum, A.S. Pikovsky, and J. Kurths, *ibid.* **78**, 4193 (1997).
- [12] R.L. Stratonovich, *Topics in the Theory of Random Noise* (Gordon and Breach, New York, 1967), Vol. 2.
- [13] P. Tass *et al.*, *Phys. Rev. Lett.* **81**, 3291 (1998); L.Q. Zhu, A. Raghun, and Y.C. Lai, *ibid.* **86**, 4017 (2001).
- [14] J.F. Heagy, T.L. Carroll, and L.M. Pecora, *Phys. Rev. E* **52**, R1253 (1995); D.J. Gauthier and J.C. Bienfang, *Phys. Rev. Lett.* **77**, 1751 (1996); A. Cenys and H. Lustfeld, *J. Phys. A* **29**, 11 (1996); C.S. Zhou and C.H. Lai, *Phys. Rev. E* **59**, R6243 (1999).
- [15] R. Benzi, A. Sutera, and A. Vulpiani, *J. Phys. A* **14**, L453 (1981); K. Wiesenfeld and F. Moss, *Nature (London)* **373**, 33 (1995); L. Gammaitoni, P. Hänggi, P. Jung, and F. Marchesoni, *Rev. Mod. Phys.* **70**, 223 (1998).
- [16] G. Hu *et al.*, *Phys. Rev. Lett.* **71**, 807 (1993); A.S. Pikovsky and J. Kurths, *ibid.* **78**, 775 (1997); G. Giacomelli, M. Giudici, S. Balle, and J.R. Tredicce, *ibid.* **84**, 3298 (2000).
- [17] L. Gammaitoni *et al.*, *Phys. Rev. Lett.* **74**, 1052 (1995).
- [18] B. Shulgin, A. Neiman, and V. Anishchenko, *Phys. Rev. Lett.* **75**, 4157 (1995).
- [19] A. Neiman *et al.*, *Phys. Rev. E* **58**, 7118 (1998).
- [20] A. Longtin and D. Chialvo, *Phys. Rev. Lett.* **81**, 4012 (1998).
- [21] F. Marino *et al.*, *Phys. Rev. Lett.* **88**, 040601 (2002).
- [22] G. Schmid, I. Goychuk, and P. Hänggi, *Europhys. Lett.* **56**, 22 (2001); P. Jung and J.W. Shuai, *ibid.* **56**, 29 (2001).
- [23] A. Neiman, L. Schimansky-Geier, A. Cornell-Bell, and F. Moss, *Phys. Rev. Lett.* **83**, 4896 (1999); B. Hu and C.S. Zhou, *Phys. Rev. E* **61**, R1001 (2000); C.S. Zhou, J. Kurths, and B. Hu, *Phys. Rev. Lett.* **87**, 098101 (2001).
- [24] C.S. Zhou *et al.*, *Phys. Rev. Lett.* **89**, 014101 (2002); C.S. Zhou and J. Kurths, *Phys. Rev. E* **65**, R040101 (2002).
- [25] A.S. Pikovsky, *Radiophys. Quantum Electron.* **27**, 576 (1984); R.V. Jensen, *Phys. Rev. E* **58**, R6907 (1998).
- [26] K. Matsumoto and I. Tsuda, *J. Stat. Phys.* **31**, 87 (1983); A.S. Pikovsky, *Phys. Lett. A* **165**, 33 (1992); L. Yu, E. Ott, and Q. Chen, *Phys. Rev. Lett.* **65**, 2935 (1990).
- [27] A. Mritan and J.R. Banavar, *Phys. Rev. Lett.* **72**, 1451 (1994).
- [28] A. Pikovsky, *Phys. Rev. Lett.* **73**, 2931 (1994).
- [29] L. Longa, E.M.F. Curado, and A.A. Oliveira, *Phys. Rev. E* **54**, R2201 (1996).
- [30] H. Herzel and J. Freund, *Phys. Rev. E* **52**, 3238 (1995); G. Malescio, *ibid.* **53**, 6551 (1996); P.M. Gade and C. Basu, *Phys. Lett. A* **217**, 21 (1996).
- [31] E. Sanchez, M.A. Matias, and V. Perez-Munuzuri, *Phys. Rev. E* **56**, 4068 (1997).
- [32] C.H. Lai and C.S. Zhou, *Europhys. Lett.* **43**, 376 (1998); R.



- Toral, C.R. Mirasso, E. Hernandez-Garcia, and O. Piro, *Chaos* **11**, 665 (2001); L. Baroni, R. Livi, and A. Torcini, *Phys. Rev. E* **63**, 036226 (2001).
- [33] C.S. Zhou and J. Kurths, *Phys. Rev. Lett.* **88**, 230602 (2002).
- [34] A.B. Neiman and D.F. Russell, *Phys. Rev. Lett.* **88**, 138103 (2002).
- [35] Z.F. Mainen and T.J. Sejnowski, *Science* **268**, 1503 (1995); A.C. Tang, A.M. Bartels, and T. Sejnowski, *Cereb. Cortex* **7**, 502 (1997).
- [36] J.A. White, J.T. Rubinstein, and A.R. Kay, *Trends Neurosci.* **23**, 1 31 (2000).
- [37] E. Schneidman, B. Freedman, and I. Segev, *Neural Comput.* **10**, 1679 (1998).
- [38] A.L. Hodgkin and A.F. Huxley, *J. Physiol. (London)* **117**, 500 (1952); E.M. Izhikevich, *Int. J. Bifurcation Chaos Appl. Sci. Eng.* **10**, 1171 (2000).
- [39] P.A.P. Moran, *Aust. J. Zool.* **1**, 291 (1953).
- [40] O.N. Bjornstad, R.A. Ims, and X. Lambin, *Trends Ecol. Evol.* **14**, 427 (1999); P.J. Hudson and I.M. Cattadori, *ibid.* **14**, 1 (1999); W.D. Koenig, *ibid.* **14**, 22 (1999).
- [41] E. Post and M.C. Forchhammer, *Nature (London)* **420**, 168 (2002).
- [42] B.T. Grenfell *et al.*, *Nature (London)* **394**, 674 (1998); B. Blasius and L. Stone, *ibid.* **406**, 846 (2000).
- [43] E. Ranta, V. Kaitala, J. Lindström, and H. Linden, *Proc. R. Soc. London, Ser. B* **262**, 113 (1995); E. Ranta, V. Kaitala, J. Lindström, and E. Helle, *Oikos* **78**, 136 (1997).
- [44] L.P. Shilnikov, *Math. USSR Sb.* **10**, 91 (1970).
- [45] U. Feudel *et al.*, *Chaos* **10**, 231 (2000).
- [46] F. Argoul, A. Arnéodo, and P. Richetti, *Phys. Lett.* **120A**, 269 (1987).
- [47] F.T. Arecchi, R. Meucci, and W. Gadomski, *Phys. Rev. Lett.* **58**, 2205 (1987); F.T. Arecchi *et al.*, *Europhys. Lett.* **6**, 677 (1988).
- [48] A. Timmermann and F.F. Jin, *Geophys. Res. Lett.* **29**, 10.1029/2001GLO13369 (2002).
- [49] C.S. Zhou, J. Kurths, E. Allaria, S. Boccaletti, R. Meucci, and F.T. Arecchi, *Phys. Rev. E* **67**, 015205 (2003).
- [50] A.N. Pisarchik, R. Meucci, and F.T. Arecchi, *Eur. Phys. J. D* **13**, 385 (2001).
- [51] J. Garcia-Ojalvo and J.M. Sancho, *Noise in Spatially Extended Systems* (Springer, New York, 1999).
- [52] C. Palenzuela *et al.*, *Europhys. Lett.* **56**, 347 (2001); C. Massoller, *Phys. Rev. Lett.* **88**, 034102 (2002).
- [53] H.A. Braun *et al.*, *Int. J. Bifurcation Chaos Appl. Sci. Eng.* **8**, 881 (1998).
- [54] C.S. Zhou and J. Kurths, *Chaos* **13**, 401 (2003).
- [55] E. Allaria, F.T. Arecchi, A. di Garbo, and R. Meucci, *Phys. Rev. Lett.* **86**, 791 (2001).
- [56] B. Lindner and L. Schimansky-Geier, *Phys. Rev. E* **61**, 6103 (2000).
- [57] C.S. Zhou, J. Kurths, and B. Hu, *Phys. Rev. E* **67**, 030101(R) (2003).